AIAA-ASME HYPERSONIC RAMJET CONFERENCE
NAVAL ORDNANCE LABORATORY, WHITE OAK, MD. APRIL 23-25, 1963

63-118

EFFECTS OF EXHAUST NOZZLE RECOMBINATION ON HYPERSONIC RAMJET PERFORMANCE

I. Experimental Investigation of Recombination in Exhaust Nozzles

by
ERWIN A. LEZBERG and LEO C. FRANCISCUS
Lewis Research Center
National Aeronautics and Space Administration
Cleveland, Ohio

63118

EFFECTS OF EXHAUST NOZZLE RECOMBINATION ON HYPERSONIC RAMJET PERFORMANCE

I. Experimental Investigation of Recombination in Exhaust Nozzles

By Erwin A. Lezberg and Leo C. Franciscus

Lewis Research Center
National Aeronautics and Space Administration
Cleveland, Ohio

63118

ABSTRACT

Experimental temperature measurements have been made, in supersonic nozzles with cone exit half-angles of 10.5° and 7°, for hydrogen-air and methane-air combustion products at stagnation temperatures up to 5400° R and pressures up to 4.5 atmospheres. The results indicate freezing in the vicinity of the nozzle throat. Comparisons of the data with an approximate freezing-point analysis and an exact calculation showed good agreement with both.

Preliminary spectral absorption measurements for the OH $^2\Sigma^+ - {}^2\Pi$ electronic transition were made by using the curve of growth to determine concentration and demonstrate feasibility of spectroscopic concentration measurements.

INTRODUCTION

Performance of hypersonic ramjets using both subsonic and supersonic combustion can be dependent throughout parts of the flight corridor on kinetic rate processes in the exhaust nozzle.

A great deal of progress has been made recently on developing computer programs for calculating nozzle performance with multiple chemical reactions (e.g., refs. 1 to 3). Calculations for the hydrogen-air system are given in references 4 to 6.

Any performance calculation using finite chemical reaction rates can be only as good as the available rate data. The extent of knowledge of kinetic rate data for the three-body recombination reactions and their temperature dependence is still very much limited. Since these reactions exert the greatest influence on performance, it is important to be able to check the kinetic calculations experimentally.

The present paper presents experimental temperature measurements on an exhaust nozzle that simulates Mach 6 flight with subsonic combustion. The pressure altitude is 95,000 to 107,000 feet for an inlet-kinetic-energy efficiency of 92 percent. In addition, feasibility of measuring hydroxyl radical concentration by spectroscopic methods is investigated; such measurements should provide more detailed knowledge of chemical kinetics in exhaust nozzles.

DESCRIPTION OF FACILITY

An alumina pebble bed was used to supply air at temperatures up to 3460° R and pressures up to 4.5 atmospheres to a water-cooled combustion chamber and nozzle. A description of the facility and basic instrumentation is given in reference 7. Both hydrogen and natural gas were used in the same fuel system. The composition of the natural gas (93 percent CH_4) is given in table I. Both fuels were supplied in cylinder trailers at pressures greater than 1000 pounds per square inch gage. They were injected

into the combustion chamber through water-cooled fuel injection tubes drilled with 148 orifices 0.040 inch in diameter. The orifices were arranged to cover approximately equal areas of the combustor cross section.

A 7° half-angle DeLaval nozzle was used for the hydrogen-air measurements. The natural-gas measurements were made with the 10.5° half-angle nozzle used in the work of reference 7.

The 7° nozzle (fig. 1) had 1/2-inch-diameter optical ports at five stations downstream of the nozzle throat. The ports were purged with air during a run to keep the quartz windows clean. Static-pressure taps were drilled normal to the nozzle wall, and wall thermocouples were mounted flush with the inside wall.

Spectral-Line-Reversal Pyrometer

A self-balancing line-reversal pyrometer, modified to use a carbon arc comparison source, was used as described in reference 8 for the natural-gas - air measurements. The hydrogen-air measurements were made with the instrument using a tungsten-ribbon-lamp reference source and modified as a single-pass instrument. With the instrument used in this way, transmission losses were considerably lower than for the double-pass instrument. The loss included only reflection loss from a spherical mirrow and the source side nozzle window. The temperature range of the pyrometer was approximately 2800° to 4700° R.

The optical diagram for the pyrometer is shown in figure 2. Light from a tungsten-ribbon lamp, which was placed off axis of a spherical mirror, was focused approximately at the center plane of the nozzle and magnified 2 times. The exit beam was refocused by a second spherical mirror on the entrance slit of the pyrometer. A negative f 4.45 lens was inserted between the pyrometer and plane mirror to collimate the light beam before it entered the instrument; the lens was adjusted so that the image of the spectrometer entrance slit was centered on the source tungsten ribbon. The spectrometer accepted a beam of light approximately 0.2 inch high and 0.06 inch wide near the center of the nozzle with a depth equal to the diameter of the sodium tracer stream.

Sodium carbonate or cesium sulfate tracer was injected at the combustor centerline in a carrier gas stream through a water-cooled probe.

The line-reversal pyrometer, source, and external optics were mounted on a base that was bolted to the table of a drill press. The table could be remotely moved up or down by a motor-driven screw. Table position was indicated by the output of a linear potentiometer on a digital voltmeter; during a run, the pyrometer optical centerline was centered successively on each nozzle window.

Hydroxyl Radical Absorption Measurements

Preliminary ultraviolet absorption measurements with the OH $^2\Sigma^+ - {}^2\Pi$ electronic transition (0,0 vibrational band beginning at 3064 A) were made by using a commercial hydrogen-discharge-lamp continuum source. Light from the source was collimated with a quartz condensing lens and chopped with a four-segment wheel driven by a synchronous motor. The beam was passed through the nozzle windows and refocused on the entrance slit of a 0.5-meter Ebert mount grating monochromator. The resolution of the monochromator with 15-micron entrance and exit slits was approximately 0.24 A, in the first order. Light from the exit slit was centered on the grid of a 1 P-28 photomultiplier tube.

The photomultiplier signal was amplified, and the direct-current level recorded by a strip-chart potentiometer. The absorption measurements were made by scanning with the monochromator and recording the spectrum of the lamp alone with a nonabsorbing gas (air) flowing through the nozzle and the spectrum of the lamp with absorbing gas (hydrogen-air combustion products) flowing through the nozzle. Since the light was chopped on the source side, light from possible OH emission from the gas was not amplified. It was necessary to record the emission spectrum of the lamp alone since the OH emission spectra was found superimposed on the hydrogen continuum.

RESULTS AND DISCUSSION

Nozzle Calibration

Effective one-dimensional area ratios were calculated for the nozzle from the measured wall static pressures during a cold airflow test. When these area ratios are corrected for boundary-layer displacement thickness (ref. 7), the calculated area ratios compare quite well with the geometric area ratios (source flow spherical cap area to sonic flow area, fig. 3). Changes in effective area ratio for the hot runs were made on the basis of calculated displacement thickness for the hot runs.

Static-Temperature Measurements for Hydrogen-Air

Reversal temperature measurements using the sodium lines centered at 5893 A were determined as a function of equivalence ratio at each of the five optical port locations in the 7° nozzle.

The measurements were made at stagnation pressures of 1.6, 3.6, and 4.5 atmospheres with an inlet air temperature range of 3000° to 3400° R. The data are shown in figures 4 to 6. The dashed lines were computed from the freezing-point analysis of part II of this paper.

Since monochromatic radiation intensity is a strong exponential function of temperature in the visible region, the instrument tends to indicate the highest temperature within the colored portion of the light path through the gas. It is noted in reference 7 (fig. 10) that combustion temperature profiles were quite poor at the lower fuel flows, probably because of poor distribution through the fuel injector. Spreading of the injected tracer, or contamination of the main airstream with sodium salts in the case of sodium line reversal, will then result in large temperature gradients along the light path and subsequent weighting of the reversal temperatures. This effect can be seen at the lowest equivalence ratios, particularly at 1.6 atmospheres.

The static temperature is shown cross plotted against area ratio for an equivalence ratio of 1.0 in figure 7 for the three stagnation pressures. The previously reported temperature measurements with a 10.5° nozzle (ref. 7) are indicated by the square symbols in figures 7(a) and 7(b). The comparison of the data with the freezing-point analysis appears to be good except at the last nozzle station, where the reversal instrument is operating close to its lower limit.

Methane-Air Measurements

Some limited temperature measurements were made with methane-air combustion products at the nozzle entrance and at area ratios of 1.23 and 1.77 with the 10.5° nozzle. The combustor temperature profile determined by traversing the powder injection probe, and reversing the Cs 4553 A spectral line, is shown in figure 8. The computed combustion temperature

of 5000° R is in excellent agreement with the central part of the profile.

The nozzle measurements are shown in figure 9, in a temperature - area-ratio plot. Both the sodium and cesium lines were used. The data scatter is indicated by the vertical bars. The theoretical curves are computed for the composition given in table I from the IBM 7090 rocket performance program of reference 9.

A comparison with the hydrogen-air results at the same stagnation pressure (fig. 7(b)) shows that the freezing points will be almost identical. This is not surprising since both systems are controlled by the same three-body recombination reactions (ref. 4). The freezing of CO would not be expected to have much influence on the temperature since the energy release due to the water-gas reaction is small compared with the recombination energy.

Hydroxyl Absorption Measurements

Absorption measurements for the OH $^2\Sigma^+ - {}^2\Pi$ electronic transition (0,0) vibrational band were made at an area ratio of 1.77 with the 10.5° nozzle. Inlet conditions for the test were an equivalence ratio of 0.9 and a stagnation pressure of 4.6 atmospheres. Measured static temperature and pressure at the measuring station were 3690° R and 0.65 atmosphere, respectively.

The first-order ultraviolet spectrum of a hydrogen-discharge lamp was scanned at 5 A per minute by using 15-micron entrance and exit slits, with and without absorbing gas in the light path. The integrated absorption was determined for 14 of the strongest lines of the band beginning at 3064 A. These were well separated from adjoining strong lines by the spectrometer.

The equivalent width W for each of these lines was then determined from the known dispersion of the spectrometer and the incident light intensity. It was given by

$$W = \int_{-\infty}^{\infty} [1 - \exp(-P_\omega X)]\,d\omega \qquad (1)$$

where P_ω is the absorption coefficient per molecule, and X is the optical depth, Nl. The symbol W represents the width of a line of rectangular cross section in which absorption from the continuum is complete.

The curve of growth gives the "growth" of the quantity W as the number of absorbers in the light path increases. The relative number of absorbers for each spectral line can be given as

$$N_{rel} = \frac{Q_r Q_v N_{K,u}}{N_{OH}} = f(2J + 1)\exp\left(-hc\omega_K/kT\right) \qquad (2)$$

where $f = FA_K/(2J + 1)$ has been determined by Oldenberg and Rieke (ref. 10) and corrected by Dwyer and Oldenberg (ref. 11). The line strength A_K and rotational wave number ω_K are taken from reference 12. The value of F, from references 10 and 11, was 3.07×10^{-4}. This has been corrected for more recent thermodynamic data on the dissociation energy of OH (ref. 13), to a value of 2.63×10^{-4}. The curve of growth has been used by Carrington (ref. 14) to redetermine the f number, and his results agree quite closely with Oldenberg's.

The experimental results have been plotted as $W(\ln 2)^{1/2}/2b_D$ against $\Sigma FA_K \exp(-hc\omega_K/kT)\ (\ln 2)^{1/2}/2\pi b_D c$. Both scales have been made nondimensional by dividing by the total width of the Doppler broadened line $2b_D/(\ln 2)^{1/2}$.

Six of the lines were overlapped with weak lines, and a correction for the line strength was applied by adding the contribution of the weaker line from equation (2). The results have been fitted to the theoretical growth curves of reference 15, by a slide fit of the abscissa scales, and the absolute number of absorbers for any given line $\ell N_{K,u}$ thus determined.

The total number of OH molecules is then given by

$$\ell N_{OH} = \left[\frac{N_K f \ell (\ln 2)^{1/2}}{2\pi b_D c}\right] \frac{2\pi b_D c}{(\ln 2)^{1/2}} \left[\frac{\exp(hc\omega_K/kT)}{FA_K}\right] Q_r Q_v \qquad (3)$$

where Q_r and Q_v are the partition functions for rotation and vibration, respectively.

The total number of absorbers was calculated as 1.75×10^{16} cm^{-3}. For the temperature and pressure at the measuring station, the mole fraction of OH is calculated as 0.0075. Computed equilibrium mole fraction was also 0.0075 for this case. The agreement is probably without much significance since the error in the f value is estimated by Oldenberg as 15 percent, and the error in the sliding fit of the experimental to the theoretical curve is about 30 percent.

The experimental curve was obtained by using strong lines. If a spectroscope of greater resolution had been available, weak lines could have been used. The fit would have been improved, since the slope is greater in the region of low absorption, and the equivalent width is independent of line shape.

CONCLUDING REMARKS

Temperature Measurements

A freezing-point approximation (part II of this paper) has shown good agreement with the measured temperatures for hydrogen-air combustion products. An exact calculation for the conditions of figure 7 has been made by Sarli (ref. 16) and is indicated by the intermediate solid line. This line was calculated for an inlet-air temperature of 3000° R for the 10.5° nozzle. Adjusting the air temperature to the mean value of 3300° R for the circled data points would increase the computed nozzle temperatures by about 60° F. No difference would be expected between the 7° and 10.5° nozzles, since freezing occurred before the exit cone and inlet and throat sections of the two nozzles were identical. A similar calculation has been shown by Ferri et al (ref. 6). Both calculations are in good agreement with the data and the approximation.

Absorption Measurements

Westenberg and Favin (ref. 4) show the insensitiveness of the gross flow parameters to changes in the reaction rates; hence measurements of temperature or pressure cannot yield precise rate data. Concentrations of several of the species in the hydrogen-air system show much greater sensitivity to changes in the reaction rates, so that concentration measurements along with temperatures can be used to check a set of reaction-rate constants.

The feasibility of spectroscopic absorption measurements for OH has been demonstrated by using the curve of growth to calculate concentrations. The method is tedious, however, and does not yield the desired precision.

The method to be used subsequently will be the line absorption technique (ref. 17). This method is not limited so severely by spectrometer resolution since the source (capillary discharge in water vapor) is essentially monochromatic with respect to each absorption line. Peak absorption is thus measured, and weak lines may be used that are not self-absorbed. A disadvantage is the fact that the shape of the line must be known. The value of a, as determined from figure 10, represents the ratio of collision to Doppler broadening and yields the information regarding line shape. Other values have been obtained, however, (refs. 14 and 18), and the best value to use will have to be resolved.

SYMBOLS

A	cross-sectional area of nozzle
A^*	critical flow area
A_K	line strength
a	ratio of collision broadening to Doppler broadening, $\frac{b_N + b_c}{b_D} (\ln 2)^{1/2}$
b_c	collision half-width, cm^{-1}
b_D	Doppler half-width of spectral line, cm^{-1}
b_N	natural half-width of spectral line, cm^{-1}
c	speed of light, cm/sec
F	$f(2J + 1)/A_K$
f	ratio of number of dispersion electrons to number of absorbers
h	Planck constant
J	rotational quantum number
k	Boltzman constant
ℓ	length, cm
N	concentration, cm^{-3}
P_ω	absorption coefficient per molecule, cm^{-2}
p	static pressure
Q_r, Q_v	partition functions for rotation and vibration
R	radial distance
T	static temperature
W	equivalent width, cm^{-1}
X	optical depth, $N\ell$, cm^{-2}
δ^*	displacement thickness
φ	equivalence ratio
ω	wave number, cm^{-1}

Subscripts:

A	air
eq	equilibrium
OH	hydroxyl radical
K	rotational level
u	upper electronic state
0	stagnation state

REFERENCES

1. Emanuel, G., and Vincenti, W. G.: Method for Calculation of the One-Dimensional Non-Equilibrium Flow of a General Gas Mixture Through a Hypersonic Nozzle. TDR-62-131, AEDC, June 1962.

2. Eschenroeder, A. Q., Boyer, D. W., and Hall, J. G.: Nonequilibium Expansions of Air with Coupled Chemical Reactions. The Phys. of Fluids, vol. 5, no. 5, May 1962.

3. Bray, K. N. C., and Appelton, J. P.: Atomic Recombination in Nozzles: Methods of Analysis for Flows with Complicated Chemistry. Rep. A.A.S.U. 166, Univ. Southampton, Apr. 1961.

4. Westenberg, A. A., and Favin, S.: Complex Chemical Kinetics in Supersonic Nozzle Flow. Paper Presented at Ninth Int. Combustion Symposium, Ithica, (N.Y.), Aug. 1962.

5. Sarli, V. J., Blackman, A. W., and Buswell, R. L.: Kinetics of Hydrogen-Air Systems. II - Calculation of Nozzle Flows for Ramjets. Paper Presented at Ninth Int. Combustion Symposium, Ithica (N.Y.), Aug. 1962.

6. Ferri, A., Libby, P. A., and Zakkay, V.: Theoretical and Experimental Investigation of Supersonic Combustion. P.I.B. ARL 62-467, Sept. 1962.

7. Lezberg, E. A., and Lancashire, R. B.: Recombination of Hydrogen-Air Combustion Products in an Exhaust Nozzle. NASA TN D-1052, 1961.

8. Buchele, D.: A Self-Balancing Line-Reversal Pyrometer. Paper Presented at Fourth Symposium on Temperature, Its Measurement and Control in Sci., and Industry, Columbus (Ohio), Mar. 27-31, 1961.

9. Zeleznik, F. J., and Gordon, S.: A General IBM 704 or 7090 Computer Program for Computation of Chemical Equilibrium Compositions, Rocket Performance, and Chapman-Jouguet Detonations. NASA TN D-1454, 1962.

10. Oldenberg, O., and Rieke, F. F.: Kinetics of OH Radicals as Determined by Their Absorption Spectrum. III. A Quantitative Test for Free OH; Probabilities of Transition. Jour. Chem. Phys., vol. 6, Aug. 1938, pp. 439-446.

11. Dwyer, R. J., and Oldenberg, O.: Jour. Chem. Phys., vol. 12, vol. 351, 1944.

12. Dieke, G. H., and Crosswhite, H. M.: The Ultraviolet Bands of OH. Bumblebee Rep. 86, The Johns Hopkins Univ., 1948.

13. Barrow, R. F., Arkiv Fysik, vol. 11, 1956, p. 281; Proc. Phys. Soc. (London), ser. A, vol. 69, 1958, p. 176.

14. Carrington, T.: Line Shape and f Value in the OH $^2\Sigma^+ - {}^2\Pi$ Transition. Jour. Chem. Phys., vol. 31, no. 5, Nov. 1959.

15. Penner, S. S., and Kavanagh, R. W.: Jour. Optical Soc. Am., vol. 43, 1953, p. 385.

16. Sarli, V. J.: Exhaust Nozzle Recombination of Dissociated Hydrogen-Air Combustion Products. Rep. A210001-1, UAC RL, Sept. 1962.

17. Kaskan, W. E.: Hydroxyl Concentrations in Rich Hydrogen-Air Flames Held on Porous Burners. Combustion and Flame, vol. 2, no. 3, Sept. 1958.

18. Kaskan, W. E.: Line Widths and Integrated Absorption Coefficients for the U.V. Bands of OH. Jour. Chem. Phys., vol. 29, 1958, p. 1420.

TABLE I. - ANALYSIS OF NATURAL-GAS FUEL

LEZBERG-8

Constituent	Volume percent
Nitrogen	1.24
Methane	92.63
Carbon dioxide	.96
Ethane	3.95
Propane	.87
Iso-butane	.10
n-butane	.16
n-pentane	.09
	100.00

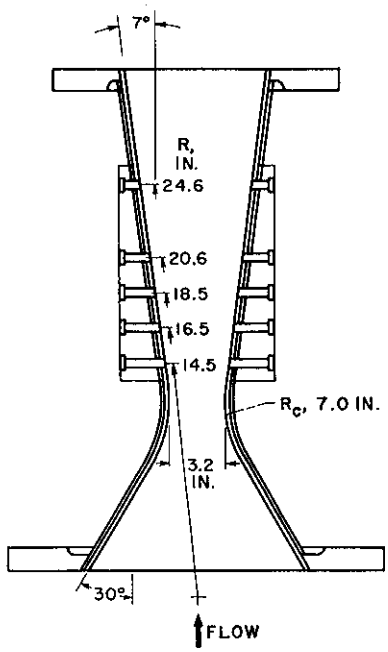

Fig. 1. Nozzle optical-port locations.

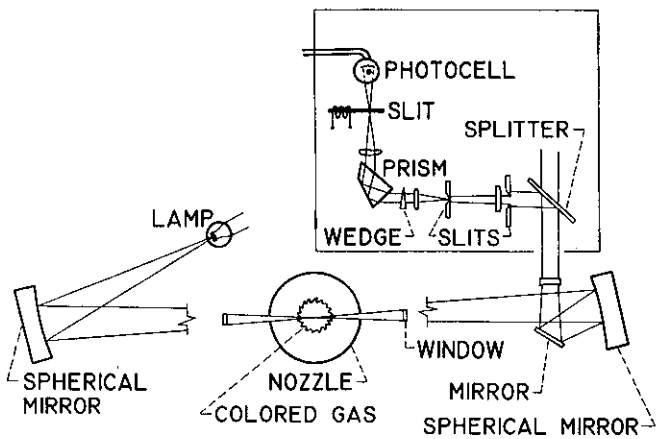

Fig. 2. Single-pass spectral-line-reversal pyrometer.

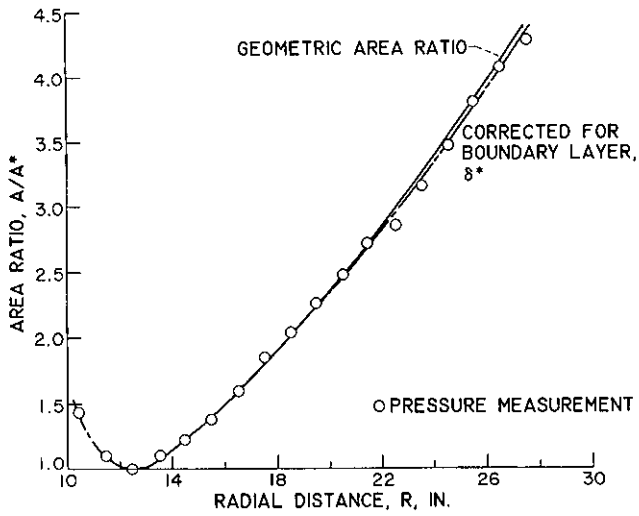

Fig. 3. One-dimensional area ratio of nozzle from cold-flow calibration.

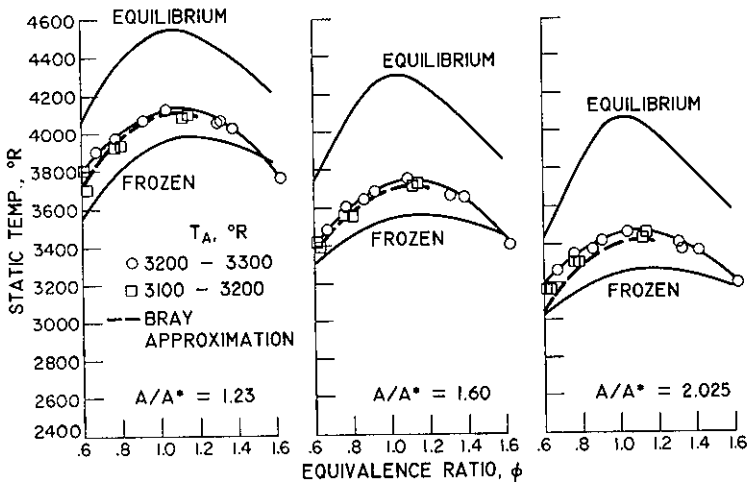

Fig. 4a. Effect of equivalence ratio on nozzle static temperature. P_0 = 1.6 ATM.

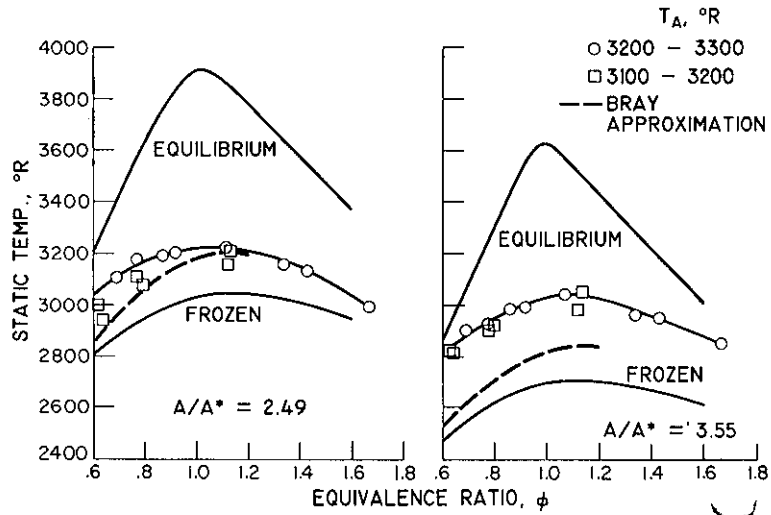

Fig. 4b. Effect of equivalence ratio on nozzle static temperature. P_0 = 1.6 ATM.

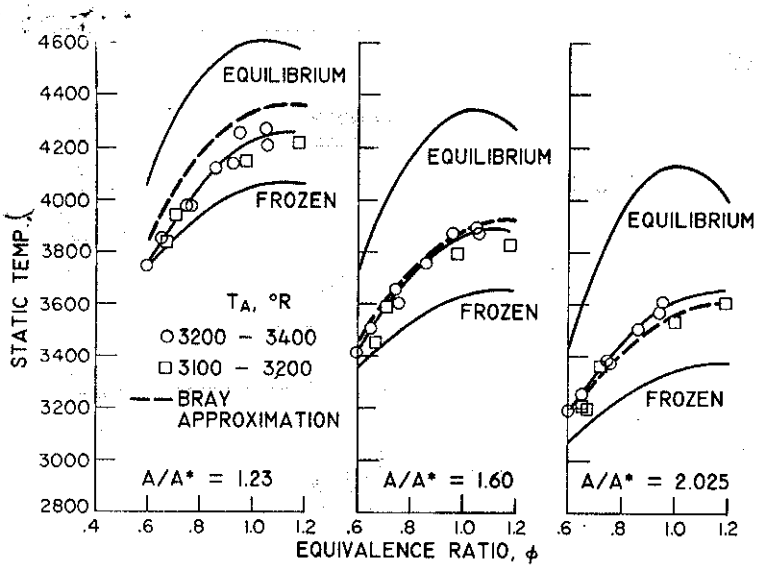

Fig. 5a. Effect of equivalence ratio on nozzle static temperature. P_0 = 3.6 ATM.

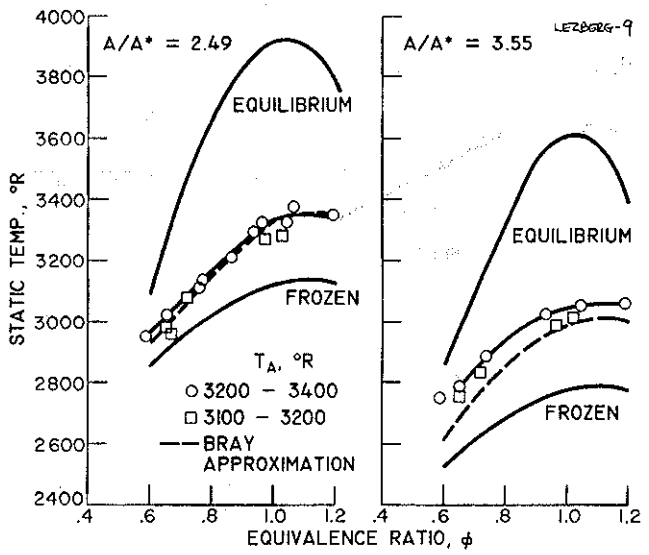

Fig. 5b. Effect of equivalence ratio on nozzle static temperature. P_0 = 3.6 ATM.

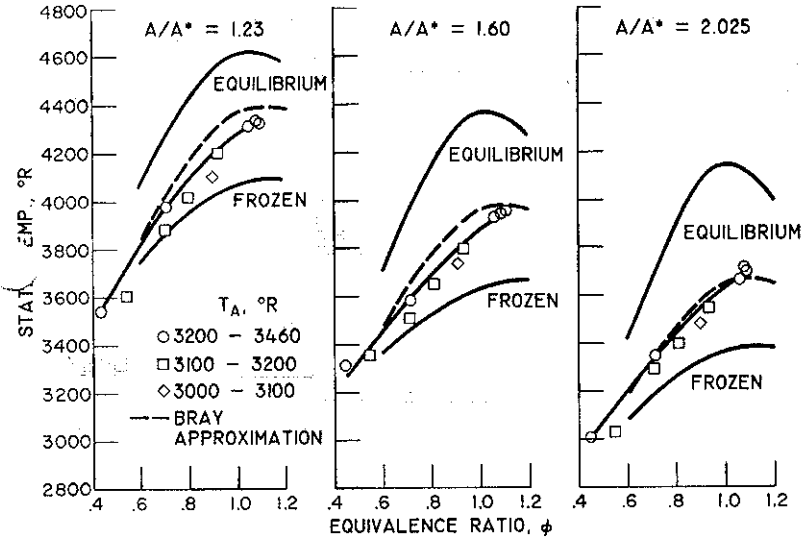

Fig. 6a. Effect of equivalence ratio on nozzle static temperature. P_0 = 4.5 ATM.

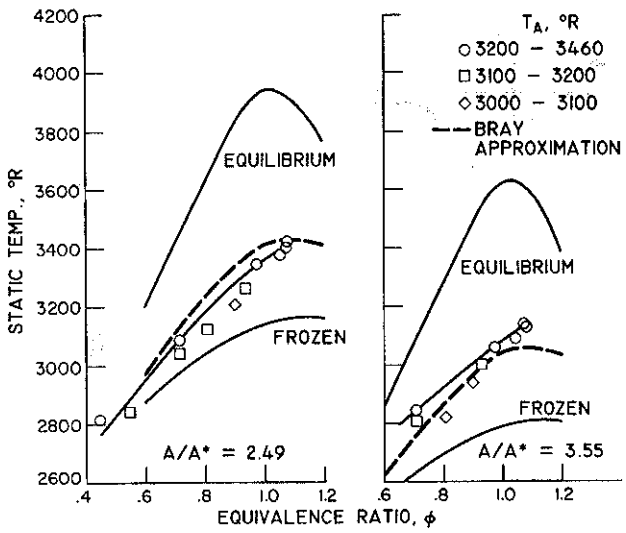

Fig. 6b. Effect of equivalence ratio on nozzle static temperature. P_0 = 4.5 ATM.

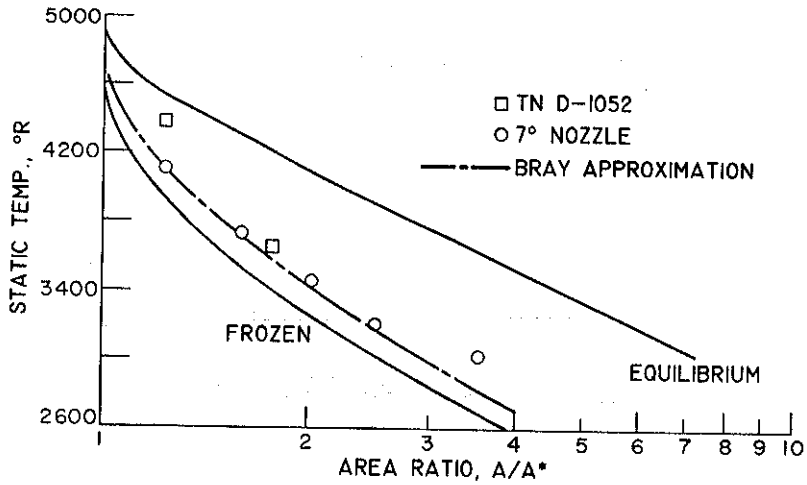

Fig. 7a. Hydrogen-air static-temperature variation with area ratio. Φ = 1.0; P_0 = 1.6 ATM; T_A = 3200° - 3300° R.

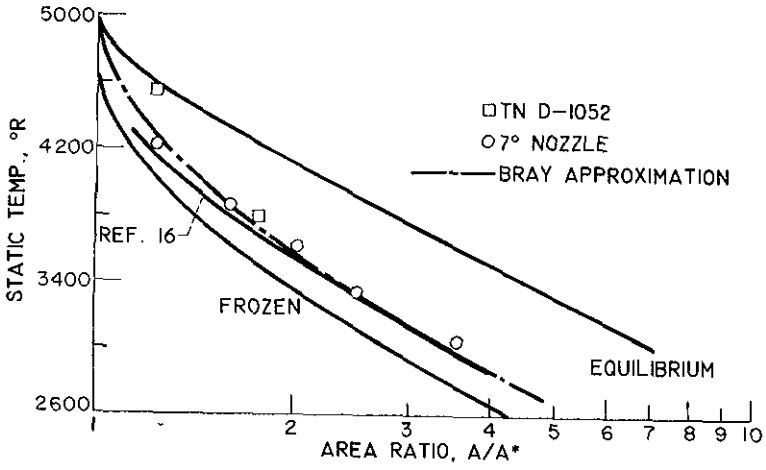

Fig. 7b. Hydrogen-air static-temperature variation with area ratio. 7° Nozzle; $\Phi = 1.0$; $P_0 = 3.6$ ATM; $T_A = 3200^0 - 3400^0$ R.

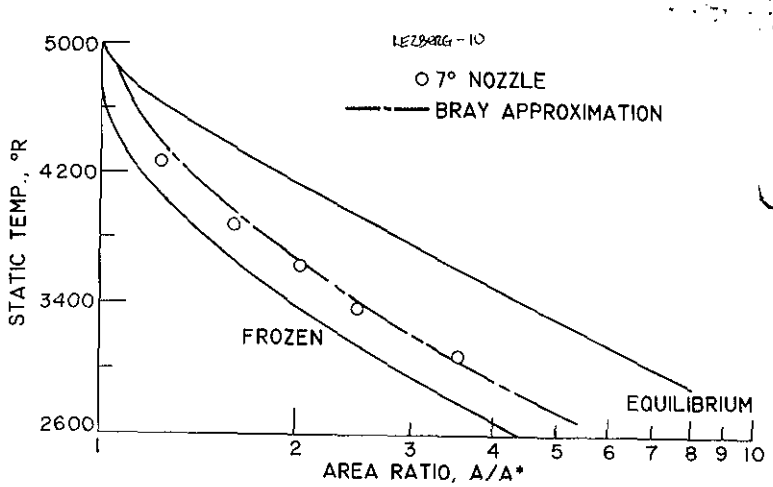

Fig. 7c. Hydrogen-air static-temperature variation with area ratio. $\Phi = 1.0$; $P_0 = 4.5$ ATM; $T_A = 3200^0 - 3460^0$ R.

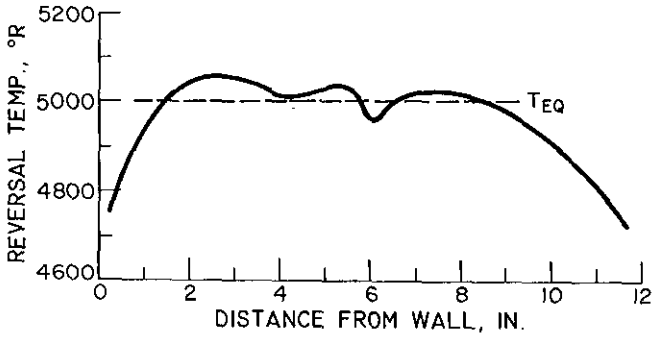

Fig. 8. Combustor temperature profile. Reversal of Cs - 4553Å line. Nat. gas fuel; $P_0 = 3.6$ ATM; $\Phi = 0.954$; $T_A = 3220^0$ R.

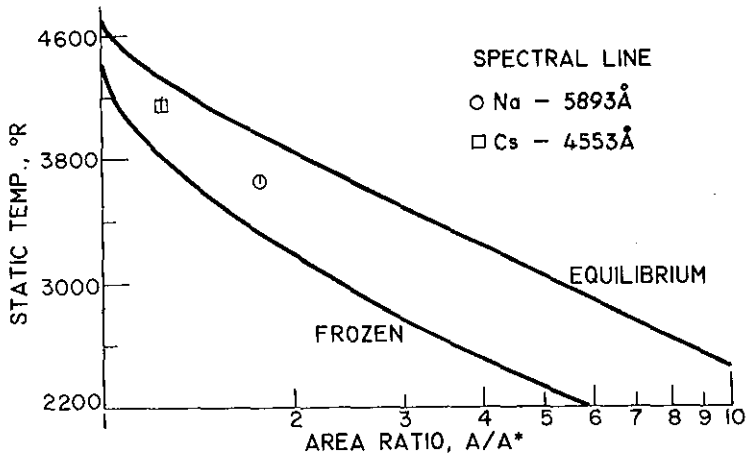

Fig. 9. Methane-air static-temperature variation with area ratio. $P_0 = 3.6$ ATM; 10.5^0 nozzle; $\Phi = 1.0$; $T_A = 2735^0 - 3135^0$ R.

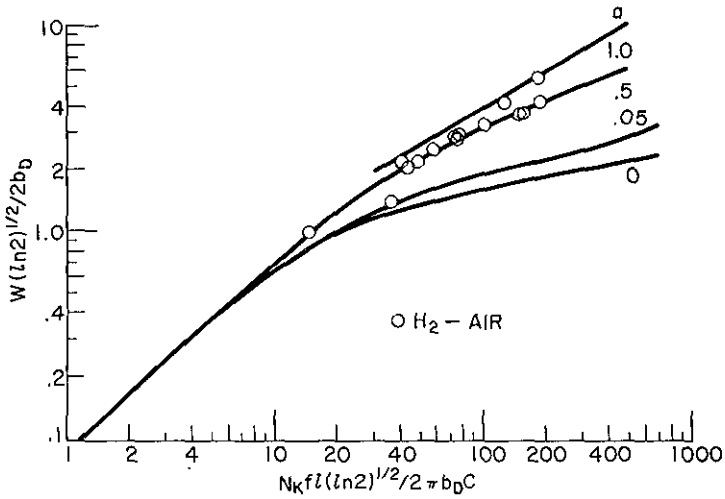

Fig. 10. Curve of growth. Absorption spectrum from H_2 continuum. OH $^2\Sigma^+ - {}^2\pi$ transition, 0-0, band. $P_0 = 4.6$ ATM; P = 0.65 ATM; T = 3690° R; $\Phi = 0.9$; $A/A^* = 1.77$.